Computational modelling of optical tweezers

Timo A. Nieminen, Norman R. Heckenberg, and Halina Rubinsztein-Dunlop

Centre for Biophotonics and Laser Science, Department of Physics,
The University of Queensland, Brisbane QLD 4072, Australia

ABSTRACT

Computational modelling of optical tweezers offers opportunities for the study of a wide range of parameters such as particle shape and composition and beam profile on the performance of the optical trap, both of which are of particular importance when applying this technique to arbitrarily shaped biological entities. In addition, models offer insight into processes that can be difficult to experimentally measure with sufficient accuracy. This can be invaluable for the proper understanding of novel effects within optical tweezers. In general, we can separate methods for computational modelling of optical tweezers into two groups: approximate methods such as geometric optics or Rayleigh scattering, and exact methods, in which the Maxwell equations are solved. We discuss the regimes of applicability of approximate methods, and consider the relative merits of various exact methods. The T-matrix method, in particular, is an attractive technique due to its efficiency for repeated calculations, and the simplicity of determining the optical force and torque. Some example numerical results are presented.

Keywords: Optical tweezers, laser trapping, light scattering, T-matrix

1. INTRODUCTION

Optical trapping, which is the trapping and manipulation of microscopic particles by a focussed laser beam or beams, is a widely used and powerful tool. The most common optical trap, the single-beam gradient trap, commonly called *optical tweezers*, consists of a laser beam strongly focussed by a lens, typically a high-numerical aperture microscope objective, with the same microscope being used to view the trapped particles.[1] The trapped particle is usually in a liquid medium, on a microscope slide. Commonly used laser sources employed for trapping range from He–Ne lasers, through Ar ion and semiconductor lasers to TiS and NdYAG lasers. Varying laser powers are used in a broad range of applications of optical tweezers—from just a few milliwatts to hundreds of mW. For most of the lasers used, when the beam is passed through the objective lens, the focal spot of the trapping beam is of the order of a micron. The trapped objects can vary in size from hundreds of nanometres to hundreds of microns.

Optical tweezers have seen deployment in a wide range of applications in biology, soft materials, microassembly, and other. As well as being used for the trapping and manipulation of a wide range of natural and artificial objects, optically trapped probes are used to measure forces on the order of piconewtons. Compared with this diverse range of experimental applications, theory and accurate computational modelling of optical tweezers has received much less attention and has remained relatively undeveloped, especially for non-spherical particles and non-Gaussian beams. In part, this is because the simple fact of trapping is sufficient for many practical applications; even for quantitative applications, where the optical trap can be calibrated by the viscous drag acting on a spherical particle, or by Brownian motion.

However, there are a number of areas where theory and computational modelling can make an important, even decisive, contribution. These include:

- **Optimising traps:** Typically one wishes to obtain maximal trapping forces with minimal power. This can be particularly important if the trapped object, or nearby objects, are susceptible to damage or death through excessive power ("opticution"). For trap parameters which can be varied, such as the size or composition of trapped microspheres, beam profile, focal spot size, etc, computational modelling can be used to explore possibilities without time-consuming or expensive trial-and-error. An extreme case would be computational modelling to aid the design of fabricated microparticles such as optical micromotors.

Further author information: Send correspondence to Timo A. Nieminen, timo@physics.uq.edu.au

Optical Trapping and Optical Micromanipulation, edited by
Kishan Dholakia, Gabriel C. Spalding, Proceedings of SPIE Vol. 5514
(SPIE, Bellingham, WA, 2004) · 0277-786X/04/$15 doi: 10.1117/12.557090

- **Validating measurement systems:** Computational modelling can be used to verify that the results obtained from measurement systems, such as trap spring constants, escape forces, or optical torques are accurate. For example, our system for the all-optical measurement of optical torques was compared with the results of modelling.[2]
- **Understanding new phenomena:** When surprising new effects are seen, computational modelling can be used to determine whether or not these new effects arise from known forces. Hypotheses concerning such effects can be incorporated into a model in order to determine the strength of such effects, and whether or not they match the observed behaviour. For example, we were able to clearly identify the mechanism acting to cause alignment of chloroplasts within an optical trap as shape birefringence.[3]

The physics of trapping is often described in terms of a gradient force, attracting dielectric particles to regions of high intensity, and a scattering force, arising from reflection and absorption, acting to push the particle out of the trap along the beam axis. More fundamentally, the optical forces arise from the transfer of momentum from the trapping beam to the particle via scattering. As electromagnetic fields can carry angular momentum as well as linear momentum, optical torques can also be exerted on particles in optical traps. If this scattering problem can be solved, then the optical force and torque can be found.

2. COMPUTATIONAL LIGHT SCATTERING

The scattering calculations required for the computational modelling of optical tweezers are, in many ways, quite straightforward. For example, the trapped particle is usually not too large compared to the wavelength, the system consists of a single scatterer, and the illumination is monochromatic. Additionally, the scatterer often has a simple geometry, for example, spherical and isotropic. Therefore, one might imagine that all that is required is to obtain a light-scattering computer code, perhaps originally written to model scattering by hydrometeors, solve the scattering problem, and hence determine the optical force and torque.

However, there are complications that prevent simple direct application of typical light-scattering codes. The most important is that optical tweezers makes use of a highly focussed laser beam, while most existing scattering codes assume plane wave illumination.

In general, computational methods for light scattering can be divided into exact and approximate methods. In the exact methods, one directly solves the Maxwell equations or the vector Helmholtz equation, while in the approximate methods, simplifying assumptions about the nature of the scatterer are made. As a result, the approximate methods are only accurate within restricted regimes (see figure 1).

Approximate methods have frequently been applied to modelling optical tweezers, with both geometric optics (which requires the smallest particle dimension to be about ten wavelengths or larger) and Rayleigh scattering (which requires that the largest dimension to be less than half the wavelength) being used. The regimes of applicability of these methods exclude the size range of particles that are commonly trapped in optical tweezers.

A diverse range of exact methods exist. That so many methods exist is indicative of the fact that no universally superior method exists; all have their various strengths and weaknesses. An important consideration for modelling optical tweezers is the efficiency of repeated calculations—characterisation of an optical trap generally requires repeated calculations to find the variation of optical force and torque with position and orientation within the trap, easily leading to thousands of calculations.

The most general exact methods involve direct time-domain solution of the Maxwell equations, using either a finite-difference (finite-difference time-domain method, or FDTD) or finite-element (finite element method, or FEM) discretisation. Both have seen limited application to modelling optical tweezers.[4–6] These methods are general and powerful, but slow. Since the entire volume of the particle (and some of the surrounding space) is discretised, these methods are also inefficient for homogeneous particles.

Another general method is the discrete-dipole approximation (DDA), also known as the coupled-dipole method. The scatterer is discretised as a collection of Rayleigh scatterers, and the problem of a single, large, possibly complex scatterer is converted into a multiple scattering problem with very simple scatterers. This has also seen limited application to the calculation of optical forces.[7] An interesting feature of this method is that it yields the force per dipole element, and hence can be used to calculate internal stresses due to the optical force.

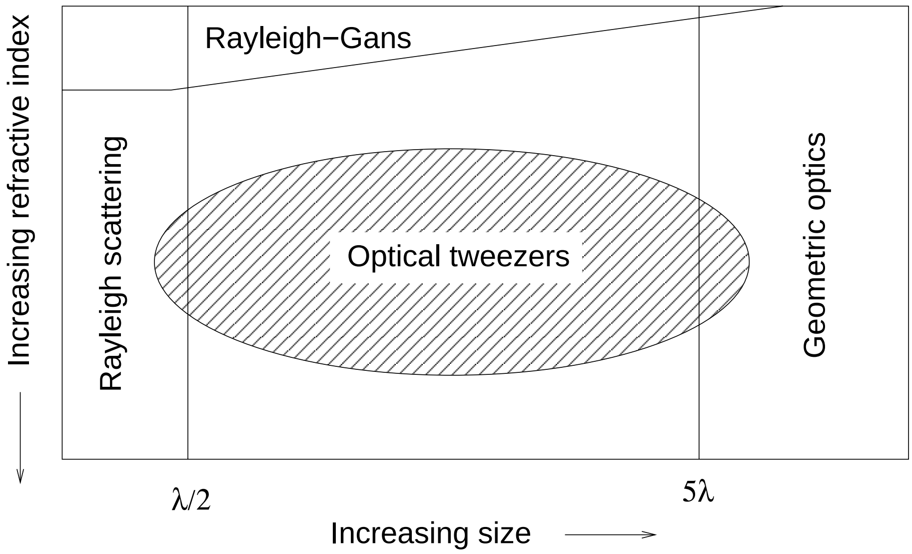

Figure 1. Regimes of applicability of approximate methods for light scattering. Particles trapped in optical tweezers are often a few wavelengths in size, and approximate methods have only limited applicability.

In general, scattering by a homogeneous scatterer can be calculated by surface methods rather than volume methods. A variety of such methods exist, such as the method of moments, the point-matching method, and various surface integral methods including the extended boundary condition method (EBCM). The surface method most commonly applied to optical tweezers is Lorenz–Mie theory,[8, 9] often called generalised Lorenz–Mie theory when non-plane wave illumination is considered. Some thorough treatments of optical tweezers via Lorenz–Mie theory have appeared.[10–15] The chief weakness of Lorenz–Mie theory is its restriction to homogeneous isotropic spheres. A limited range of other shapes, such as spheroids, can also be treated in a similar manner.[16, 17]

A useful feature of Lorenz–Mie theory is that the incident and scattered waves are expanded in a modal representation, using vector spherical wavefunctions (see next section), and the Mie coefficients relating the two sets of modes are independent of the details of the illumination, and only need to be calculated once for a particular particle for one wavelength. While Lorenz–Mie theory is restricted to a spherical geometry where an analytical solution for the coefficients can be found, this is not a requirement for the general formalism to be useful. Such a description of the scattering properties of the particle is called the T-matrix formalism, and it proves to be a highly efficient method of modelling optical tweezers. The key to this efficiency is that, just as the Mie coefficients are independent of the illumination, so is the T-matrix describing the relationship between the incident and scattered fields. Thus, the T-matrix only needs to be calculated once, and can then be used for repeated calculations. It also turns out to be very simple to calculate the optical force and torque in the T-matrix method, with no numerical integration of the Maxwell stress tensor being required. For these reasons, it is ideally suited for the modelling of optical tweezers, and is our method of choice.

A thorough review by Kahnert covers most of the exact methods mentioned above, and their theoretical foundations.[18]

3. *T*-MATRIX DESCRIPTION OF SCATTERING

The T-matrix method in wave scattering involves writing the relationship between the wave incident upon a scatterer, expanded in terms of a sufficiently complete basis set of functions $\psi_n^{(\mathrm{inc})}$, where n is mode index labelling the functions, each of which is a solution of the Helmholtz equation,

$$U_{\rm inc} = \sum_n^{\infty} a_n \psi_n^{(\rm inc)}, \tag{1}$$

where a_n are the expansion coefficients for the incident wave, and the scattered wave, also expanded in terms of a basis set $\psi_k^{(\rm scat)}$,

$$U_{\rm scat} = \sum_k^{\infty} p_k \psi_k^{(\rm scat)}, \tag{2}$$

where p_k are the expansion coefficients for the scattered wave, is written as a simple matrix equation

$$p_k = \sum_n^{\infty} T_{kn} a_n \tag{3}$$

or, in more concise notation,

$$\mathbf{P} = \mathbf{TA} \tag{4}$$

where T_{kn} are the elements of the T-matrix.

The T-matrix method can be used for scalar waves or vector waves in a variety of geometries, with the only restrictions being that the geometry of the problem permits expansion of the waves as discrete series in terms of the chosen basis, that the response of the scatterer to the incident wave is linear, and that the expansion series for the waves can be truncated at a finite number of terms. Since here we are interested in electromagnetic scattering, the functions making up the basis must be divergence-free solutions of the vector Helmholtz equation.

The T-matrix depends only on the properties of the particle—its composition, size, shape, and orientation—and the wavelength, and is otherwise independent of the incident field. This means that for any particular particle, the T-matrix only needs to be calculated once, and can then be used for repeated calculations. This is the key point that makes this an attractive method for modelling optical tweezers, providing a significant advantage over many other methods of calculating scattering where the entire calculation needs to be repeated.

For other geometries, other sets of eigenfunctions, such as cylindrical wavefunctions (for scatterers of infinite length in one dimension), or a Floquet expansion (planar periodic scatterers), are more appropriate. There is no requirement that the modes into which the incident and scattered fields are expanded be the same, or even similar.

In general, one calculates the T-matrix, although it is conceivable that it might be measured experimentally.

3.1. Incident and scattered wave expansions

The natural choice of coordinate system for optical tweezers is spherical coordinates centered on the trapped particle. Thus, the incoming and outgoing fields can be expanded in terms of incoming and outgoing vector spherical wavefunctions (VSWFs):

$$\mathbf{E}_{\rm in} = \sum_{n=1}^{\infty} \sum_{m=-n}^{n} a_{nm} \mathbf{M}_{nm}^{(2)}(k\mathbf{r}) + b_{nm} \mathbf{N}_{nm}^{(2)}(k\mathbf{r}), \tag{5}$$

$$\mathbf{E}_{\rm out} = \sum_{n=1}^{\infty} \sum_{m=-n}^{n} p_{nm} \mathbf{M}_{nm}^{(1)}(k\mathbf{r}) + q_{nm} \mathbf{N}_{nm}^{(1)}(k\mathbf{r}). \tag{6}$$

where the VSWFs are

$$\begin{aligned} \mathbf{M}_{nm}^{(1,2)}(k\mathbf{r}) &= N_n h_n^{(1,2)}(kr) \mathbf{C}_{nm}(\theta,\phi) \qquad (7) \\ \mathbf{N}_{nm}^{(1,2)}(k\mathbf{r}) &= \frac{h_n^{(1,2)}(kr)}{krN_n} \mathbf{P}_{nm}(\theta,\phi) + N_n \left(h_{n-1}^{(1,2)}(kr) - \frac{n h_n^{(1,2)}(kr)}{kr} \right) \mathbf{B}_{nm}(\theta,\phi) \end{aligned}$$

where $h_n^{(1,2)}(kr)$ are spherical Hankel functions of the first and second kind, $N_n = [n(n+1)]^{-1/2}$ are normalization constants, and $\mathbf{B}_{nm}(\theta,\phi) = \mathbf{r}\nabla Y_n^m(\theta,\phi)$, $\mathbf{C}_{nm}(\theta,\phi) = \nabla \times (\mathbf{r}Y_n^m(\theta,\phi))$, and $\mathbf{P}_{nm}(\theta,\phi) = \hat{\mathbf{r}}Y_n^m(\theta,\phi)$ are the vector spherical harmonics,[19–22] and $Y_n^m(\theta,\phi)$ are normalized scalar spherical harmonics. The usual polar spherical coordinates are used, where θ is the co-latitude measured from the $+z$ axis, and ϕ is the azimuth, measured from the $+x$ axis towards the $+y$ axis.

$\mathbf{M}_{nm}^{(1)}$ and $\mathbf{N}_{nm}^{(1)}$ are outward-propagating TE and TM multipole fields, while $\mathbf{M}_{nm}^{(2)}$ and $\mathbf{N}_{nm}^{(2)}$ are the corresponding inward-propagating multipole fields. Since these wavefunctions are purely incoming and purely outgoing, each has a singularity at the origin. Since fields that are free of singularities are of interest, it is useful to define the singularity-free regular vector spherical wavefunctions:

$$\mathbf{RgM}_{nm}(k\mathrm{r}) = \tfrac{1}{2}[\mathbf{M}_{nm}^{(1)}(k\mathrm{r}) + \mathbf{M}_{nm}^{(2)}(k\mathrm{r})], \tag{8}$$

$$\mathbf{RgN}_{nm}(k\mathrm{r}) = \tfrac{1}{2}[\mathbf{N}_{nm}^{(1)}(k\mathrm{r}) + \mathbf{N}_{nm}^{(2)}(k\mathrm{r})]. \tag{9}$$

Although it is usual to expand the incident field in terms of the regular VSWFs, and the scattered field in terms of outgoing VSWFs, this results in both the incident and scattered waves carrying momentum and angular momentum away from the system. Since we are primarily interested in the transport of momentum and angular momentum by the fields (and energy, too, if the particle is absorbing), a separation of the total field into purely incoming and outgoing portions gives a clearer picture of these transpost properties. It should be kept in mind that the incoming field is not actually the incident field, although it does uniquely specify the incident field, and the outgoing field is a combination of the outgoing incident field and the scattered field.

This still leaves open the exact method by which the VSWF expansion of the incident field should be found. It is possible to simply use an integral transform,[12, 13] but other methods are available as well. Our method of choice uses an over-determined point-matching scheme,[23] providing stable and robust numerical performance and convergence. A very fast method is the localised approximation.[14, 15, 24–26] Some caution is in order if one wishes to begin with a standard paraxial laser beam, or beam with higher-order corrections for non-paraxiality.[23] These problems arise from standard descriptions of laser beams not being solutions to the Maxwell equations, whereas the VSWF expansion is a solution.

Since one generally desires to calculate the force and torque for the same particle in the same trapping beam, but at different positions or orientations, we can make use of the properties of the VSWFs under translation[27–29] or rotation.[30] It is sufficient to find the VSWF expansion of the incident beam for a single origin and orientation, and then use translations and rotations to find the new VSWF expansions about other points.[23, 31] Since the transformation matrices for rotation and translations along the z-axis are sparse, while the transformation matrices for arbitrary translations are full, the most efficient way to carry out an arbitrary translation is by a combination of rotation and axial translation. The transformation matrices for both rotations and axial translations can be efficiently computed using recursive methods.[28–30]

3.2. Optical force and torque

The *torque efficiency*, or normalized torque, about the z-axis acting on a scatterer is

$$\tau_z = \sum_{n=1}^{\infty} \sum_{m=-n}^{n} m(|a_{nm}|^2 + |b_{nm}|^2 - |p_{nm}|^2 - |q_{nm}|^2)/P \tag{10}$$

in units of $\hbar$ per photon, where

$$P = \sum_{n=1}^{\infty} \sum_{m=-n}^{n} |a_{nm}|^2 + |b_{nm}|^2 \tag{11}$$

is proportional to the incident power (omitting a unit conversion factor which will depend on whether SI, Gaussian, or other units are used). This torque includes contributions from both spin and orbital components;

the normalized spin torque about the z-axis is given by[32]

$$\begin{aligned}\sigma_z &= \frac{1}{P}\sum_{n=1}^{\infty}\sum_{m=-n}^{n}\frac{m}{n(n+1)}\times \\ &(|a_{nm}|^2+|b_{nm}|^2-|p_{nm}|^2-|q_{nm}|^2) \\ &-\frac{2}{n+1}\left[\frac{n(n+2)(n-m+1)(n+m+1)}{(2n+1)(2n+3)}\right]^{\frac{1}{2}} \\ &\times\mathrm{Im}(a_{nm}b^\star_{n+1,m}+b_{nm}a^\star_{n+1,m} \\ &\qquad -p_{nm}q^\star_{n+1,m}-q_{nm}p^\star_{n+1,m}).\end{aligned} \tag{12}$$

The remainder of the torque is the orbital contribution. The axial trapping efficiency Q is[32]

$$\begin{aligned}Q &= \frac{2}{P}\sum_{n=1}^{\infty}\sum_{m=-n}^{n}\frac{m}{n(n+1)}\mathrm{Re}(a^\star_{nm}b_{nm}-p^\star_{nm}q_{nm}) \\ &-\frac{1}{n+1}\left[\frac{n(n+2)(n-m+1)(n+m+1)}{(2n+1)(2n+3)}\right]^{\frac{1}{2}} \\ &\times\mathrm{Re}(a_{nm}a^\star_{n+1,m}+b_{nm}b^\star_{n+1,m} \\ &\qquad -p_{nm}p^\star_{n+1,m}-q_{nm}q^\star_{n+1,m})\end{aligned} \tag{13}$$

in units of $\hbar k$ per photon.

We use the same formulae to calculate the x and y components of the optical force and torque, using 90° rotations of the coordinate system.[30] It is also possible to directly calculate the x and y components using similar, but more complicated, formulae.[33]

3.3. Calculation of the T-matrix

Most implementations of the T-matrix method use the extended boundary condition method (EBCM), also called the null field method, to calculate the T-matrix. This is so widespread that the T-matrix method and the EBCM are sometimes considered to be inseparable, and the terms are sometimes used interchangeably. However, from the description above, it is clear that the T-matrix formalism is independent of the actual method used to calculate the T-matrix.[18, 34]

A number of alternative methods have been used for the calculation of T-matrices.[34–37] Notably, the DDA method used by Mackowski[36] is applicable to inhomogenous particles of arbitrary geometries.

Our own calculations have made use of both the EBCM and a generalised point-matching method.[34] A number of T-matrix codes are available publicly, and could be used as a starting point by the interested reader.[38, 39]

4. EXAMPLE RESULTS

As a demonstration of the methods described above, we calculate the dependence of the trapping forces on the radius of a trapped sphere. The sphere is nonabsorbing and nonmagnetic, with a refractive index of 1.6, and is trapped in water, with refractive index 1.34. The spheres are assumed to be neutrally buoyant. We compare the optical forces exerted on the sphere by a Gaussian TEM_{00} beam and a Laguerre–Gaussian LG_{03} beam. The Gaussian beam has a convergence angle of 45°, while the LG beam is assumed to have the same waist radius parameter w_0 when incident on the lens (and is therefore somewhat wider, and more convergent). The sphere is assumed to remain on the beam axis. For small spheres in the LG_{03} beam, this position will be an unstable equilbrium in the radial direction, as such spheres are stably trapped in the bright ring, rather than on the beam axis. The equilbrium point is stable against movement in the axial direction for all sizes of spheres. The results of these calculations are shown in figures 2–4. Notably, the LG beam results in a much higher spring constant and axial escape force. It can also be seen that for small spheres in the LG beam, which lie within the central dark region of the beam, the optical force is small. The sphere trapped in the Gaussian beam shows a strong

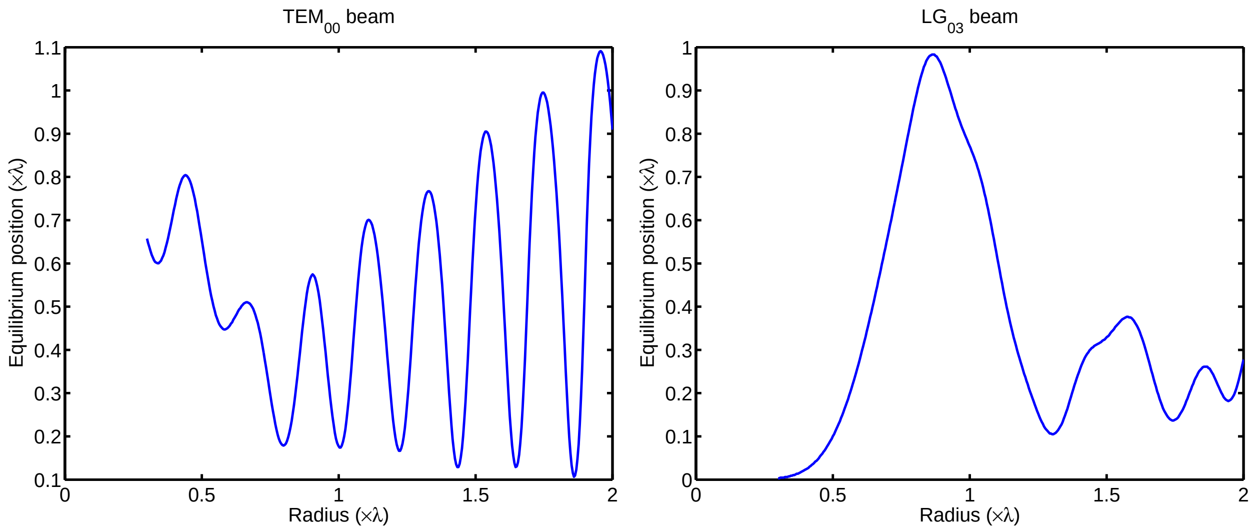

Figure 2. The equilibrium position at which a neutrally buoyant sphere is trapped is shown. For a trap with the objective above the sample, this will be distance below the focal plane that the centre of the sphere will lie. For small spheres in the LG_{03} beam, the equilibrium is radially unstable, as such spheres are stably trapped in the bright ring, rather than on the beam axis. The trapping forces result in a stable equilibrium in the axial direction for all sizes of spheres.

modulation of the optical force caused by interference between light reflected from the front and back surfaces of the sphere, akin to thin-film interference.[12, 13] This effect is not seen in geometric optics calculations since phase and interference effects are ignored in that approximation. A similar, but less distinct, effect is seen in the trapping by the LG beam as well when the particle is large enough to intercept the bright ring of the beam.

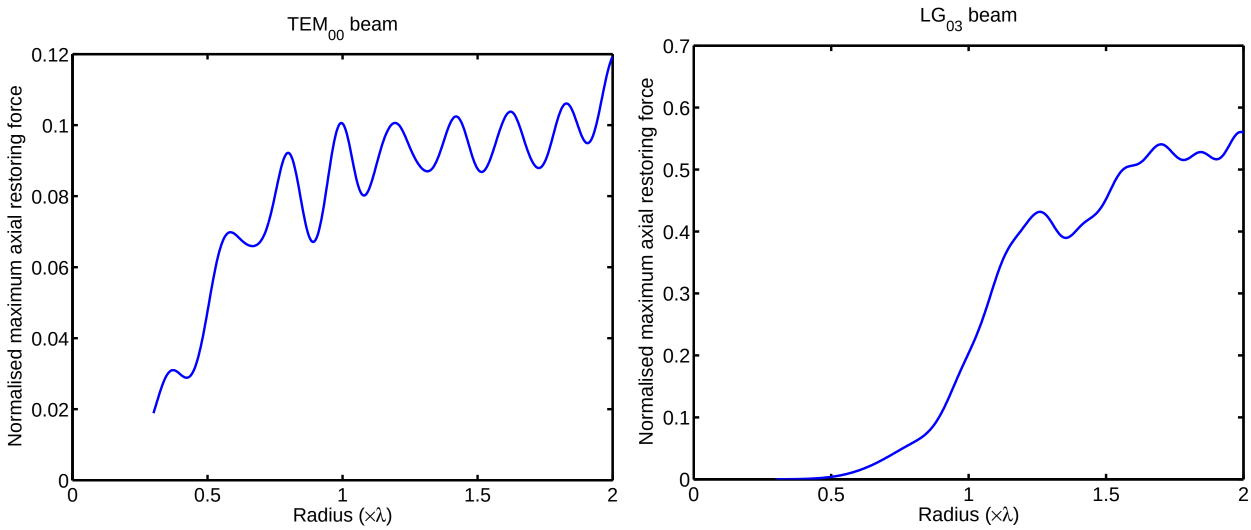

Figure 3. Axial escape force.

We have also used the same computer codes to model the trapping and rotation of non-spherical particles such as chloroplasts[3] and glass rods.[2] The calculated results agree well with experimentally measured torques.

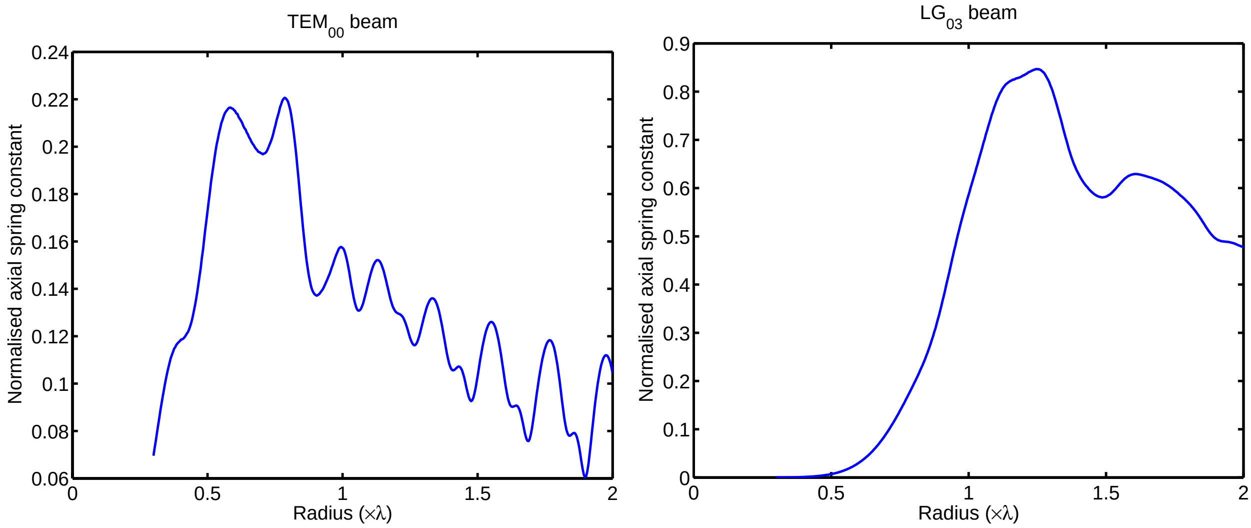

Figure 4. Axial spring constant.

5. NON-OPTICAL FORCES

A number of non-optical forces will act on the particle. Buoyancy and gravity are constant and are simply dealt with. The other important effects are viscous drag and Brownian motion. If the particle is stationary and not rotating, then viscous drag will be zero. If the particle is moving, its motion in the surrounding fluid is generally completely dominated by viscous drag—Reynolds numbers of about 10^{-5} to 10^{-3} are typical, and inertial effects are negligible. The time taken to reach terminal speed will typically be very short, on the order of 10^{-6} s or less, and simulations of the dynamics can assume that $\dot{\mathbf{r}} \propto \mathbf{F}$ instead of $\ddot{\mathbf{r}} \propto \mathbf{F}$. Since the Reynolds numbers are so low, Stoke's Law provides an excellent approximation for the drag, if the particle is spherical, and not too close to an interface.

The modelling of the dynamics of an arbitrary particle remains a formidable task, although for many purposes it is likely to be sufficient to assume the drag on the particle is the same as that on an equivalent sphere or ellipsoid.

6. CONCLUSION

We have reviewed a variety of methods that are available for the computational modelling of optical tweezers, and covered our method of choice, the T-matrix method, in more detail. The T-matrix method is highly suited for modelling optical tweezers since it is very efficient for large numbers of repeated calculations such as are required to characterise a trap. This method is applicable to arbitrary particles, including inhomogeneous, anisotropic, and geometrically complex particles.

REFERENCES

1. A. Ashkin, J. M. Dziedzic, J. E. Bjorkholm, and S. Chu, "Observation of a single-beam gradient force optical trap for dielectric particles," *Optics Letters* **11**, pp. 288–290, 1986.
2. A. I. Bishop, T. A. Nieminen, N. R. Heckenberg, and H. Rubinsztein-Dunlop, "Optical application and measurement of torque on microparticles of isotropic nonabsorbing material," *Physical Review A* **68**, p. 033802, 2003.
3. S. Bayoudh, T. A. Nieminen, N. R. Heckenberg, and H. Rubinsztein-Dunlop, "Orientation of biological cells using plane polarised Gaussian beam optical tweezers," *Journal of Modern Optics* **50**(10), pp. 1581–1590, 2003.

4. D. A. White, "Vector finite element modeling of optical tweezers," *Computer Physics Communications* **128**, pp. 558–564, 2000.
5. D. A. White, "Numerical modeling of optical gradient traps using the vector finite element method," *Journal of Computational Physics* **159**, pp. 13–37, 2000.
6. W. L. Collett, C. A. Ventrice, and S. M. Mahajan, "Electromagnetic wave technique to determine radiation torque on micromachines driven by light," *Applied Physics Letters* **82**, pp. 2730–2732, 2003.
7. A. G. Hoekstra, M. Frijlink, L. B. F. M. Waters, and P. M. A. Sloot, "Radiation forces in the discrete-dipole approximation," *Journal of the Optical Society of America A* **18**, pp. 1944–1953, 2001.
8. L. Lorenz, "Lysbevægelsen i og uden for en af plane Lysbølger belyst Kugle," *Videnskabernes Selskabs Skrifter* **6**, pp. 2–62, 1890.
9. G. Mie, "Beiträge zur Optik trüber Medien, speziell kolloidaler Metallösungen," *Annalen der Physik* **25**(3), pp. 377–445, 1908.
10. K. F. Ren, G. Gréhan, and G. Gouesbet, "Prediction of reverse radiation pressure by generalized Lorenz-Mie theory," *Applied Optics* **35**, pp. 2702–2710, 1996.
11. T. Wohland, A. Rosin, and E. H. K. Stelzer, "Theoretical determination of the influence of the polarization on forces exerted by optical tweezers," *Optik* **102**, pp. 181–190, 1996.
12. P. A. Maia Neto and H. M. Nussenzweig, "Theory of optical tweezers," *Europhysics Letters* **50**, pp. 702–708, 2000.
13. A. Mazolli, P. A. Maia Neto, and H. M. Nussenzveig, "Theory of trapping forces in optical tweezers," *Proceedings of the Royal Society of London A* **459**, pp. 3021–3041, 2003.
14. J. A. Lock, "Calculation of the radiation trapping force for laser tweezers by use of generalized Lorenz–Mie theory. I. Localized model description of an on-axis tightly focused laser beam with spherical aberration," *Applied Optics* **43**, pp. 2532–2544, 2004.
15. J. A. Lock, "Calculation of the radiation trapping force for laser tweezers by use of generalized Lorenz–Mie theory. II. On-axis trapping force," *Applied Optics* **43**, pp. 2545–2554, 2004.
16. Y. Han and Z. Wu, "Scattering of a spheroidal particle illuminated by a Gaussian beam," *Applied Optics* **40**, pp. 2501–2509, 2001.
17. Y. Han, G. Gréhan, and G. Gouesbet, "Generalized Lorenz–Mie theory for a spheroidal particle with off-axis Gaussian-beam illumination," *Applied Optics* **42**, pp. 6621–6629, 2003.
18. F. M. Kahnert, "Numerical methods in electromagnetic scattering theory," *Journal of Quantitative Spectroscopy and Radiative Transfer* **79–80**, pp. 775–824, 2003.
19. M. I. Mishchenko, J. W. Hovenier, and L. D. Travis, eds., *Light scattering by nonspherical particles: theory, measurements, and applications*, Academic Press, San Diego, 2000.
20. P. C. Waterman, "Symmetry, unitarity, and geometry in electromagnetic scattering," *Physical Review D* **3**, pp. 825–839, 1971.
21. M. I. Mishchenko, "Light scattering by randomly oriented axially symmetric particles," *Journal of the Optical Society of America A* **8**, pp. 871–882, 1991.
22. J. D. Jackson, *Classical Electrodynamics*, John Wiley, New York, 3rd ed., 1999.
23. T. A. Nieminen, H. Rubinsztein-Dunlop, and N. R. Heckenberg, "Multipole expansion of strongly focussed laser beams," *Journal of Quantitative Spectroscopy and Radiative Transfer* **79-80**, pp. 1005–1017, 2003.
24. G. Gouesbet, J. A. Lock, and G. Gréhan, "Partial-wave representations of laser beams for use in light-scattering calculations," *Applied Optics* **34**, pp. 2133–2143, 1995.
25. G. Gouesbet, "Exact description of arbitrary-shaped beams for use in light-scattering theories," *Journal of the Optical Society of America A* **13**, pp. 2434–2440, 1996.
26. G. Gouesbet, "Validity of the localized approximation for arbitrary shaped beams in the generalized Lorenz-Mie theory for spheres," *Journal of the Optical Society of America A* **16**, pp. 1641–1650, 1999.
27. B. C. Brock, "Using vector spherical harmonics to compute antenna mutual impedance from measured or computed fields," Sandia report SAND2000-2217-Revised, Sandia National Laboratories, Albuquerque, New Mexico, USA, 2001.

28. G. Videen, "Light scattering from a sphere near a plane interface," in *Light Scattering from Microstructures*, F. Moreno and F. González, eds., *Lecture Notes in Physics*(534), ch. 5, pp. 81–96, Springer-Verlag, Berlin, 2000.
29. N. A. Gumerov and R. Duraiswami, "Recursions for the computation of multipole translation and rotation coefficients for the 3-D Helmholtz equation," *SIAM Journal on Scientific Computing* **25**(4), pp. 1344–1381, 2003.
30. C. H. Choi, J. Ivanic, M. S. Gordon, and K. Ruedenberg, "Rapid and stable determination of rotation matrices between spherical harmonics by direct recursion," *Journal of Chemical Physics* **111**, pp. 8825–8831, 1999.
31. A. Doicu and T. Wriedt, "Computation of the beam-shape coefficients in the generalized Lorenz-Mie theory by using the translational addition theorem for spherical vector wave functions," *Applied Optics* **36**, pp. 2971–2978, 1997.
32. J. H. Crichton and P. L. Marston, "The measurable distinction between the spin and orbital angular momenta of electromagnetic radiation," *Electronic Journal of Differential Equations* **Conf. 04**, pp. 37–50, 2000.
33. Ø. Farsund and B. U. Felderhof, "Force, torque, and absorbed energy for a body of arbitrary shape and constitution in an electromagnetic radiation field," *Physica A* **227**, pp. 108–130, 1996.
34. T. A. Nieminen, H. Rubinsztein-Dunlop, and N. R. Heckenberg, "Calculation of the T-matrix: general considerations and application of the point-matching method," *Journal of Quantitative Spectroscopy and Radiative Transfer* **79-80**, pp. 1019–1029, 2003.
35. L. Gürel and W. C. Chew, "A recursive T-matrix algorithm for strips and patches," *Radio Science* **27**, pp. 387–401, 1992.
36. D. W. Mackowski, "Discrete dipole moment method for calculation of the t matrix for nonspherical particles," *Journal of the Optical Society of America A* **19**, pp. 881–893, 2002.
37. P. A. Martin, "On connections between boundary integral equations and t-matrix methods," *Engineering Analysis with Boundary Elements* **27**, pp. 771–777, 2003.
38. `http://www.t-matrix.de/`.
39. `http://www.giss.nasa.gov/~crmim/`.